2nd Mediterranean Conference on Fracture and Structural Integrity

On Mode I crack mechanism in the puncturing of soft tissues

Andrea Spagnoli[a,*], Roberto Brighenti[a], Riccardo Alberini[a], Matteo Montanari[a], Michele Terzano[b]

[a]*Dipartimento di Ingegneria e Architettura, Università di Parma, Parco Area delle Scienze 181/A, 43124 Parma, Italy*
[b]*Institute of Biomechanics, Graz University of Technology, Stremayrgasse 16/II, 8010 Graz, Austria*

Abstract

In the present paper, the mechanics of puncturing is studied with refer to a foreign tool penetrating a soft (nearly incompressible) target solid. The penetrating tool is here described by a sharp tipped rigid needle with a circular cross section. Puncturing can be characterised as a Mode I fracture process, which is here analytically described by a two-dimensional model related to the plane normal to the penetration axis. It is shown that the force required for the onset of needle penetration is dependent on two energy contributions, that is, the strain energy stored in the target solid and the energy consumed in Mode I crack propagation. Such a penetration force is analytically demonstrated to be dependent on the fracture toughness of the material, its elastic modulus, and the sharpness of the penetrating tool.

Keywords: cutting; puncturing; soft material; sharpness; fracture mechanics.

1. Introduction

Cutting and puncturing phenomena are characterised by complex mechanisms of progressive penetration of a stiff tool into a target soft material. The analysis and experimental measurements of the penetration forces are of great interest for scientific speculations as well as engineering applications, e.g. concerning food industry, robotic surgical operations, experimental testing and biological puncture systems (Frick et al., 2001; DiMaio and Salcudean, 2003; McGorry et al., 2003; Goh et al., 2005; Takabi and Tai, 2017; Anderson, 2018; Kundanati et al., 2020; Terzano et al., 2020, 2021). Puncture testing can also specifically used for the characterization of tissue-mimicking composites formed by additive manufacturing (e.g. see Bezek et al. (2022)). The behaviour of soft materials is considerably different from that of strong ductile solids, such as metals, soils or hard polymers, and the essential difference lies in the fracture mechanics of soft matter.

---

* Corresponding author. Tel.: +39 0521 905927 ; fax: +39 0521 905924.
E-mail address: andrea.spagnoli@unipr.it

Depending on the technique and the geometry of the penetrating tool, the mechanics of cutting and of puncturing is greatly diversified, although the process occurring at the tip of the tool is mainly a question related to the fracture mechanics of the target material. Fracture in soft materials involves large deformation prior to cracking, non-linear material behaviour, and possibly rate-dependent effects, and the emerging picture greatly differs from the linear elastic fracture mechanics (LEFM). Due to the highly deformed region and severe crack blunting occurring locally at tip, the notion of a single parameter characterisation to describe fracture, on which the whole LEFM is grounded, needs to be revised (Williams, 2015). Moreover, the local large deformation leads to a decrease in the strain localisation around the crack tip, contributing to enhanced fracture resistance and defect tolerance (Brighenti et al., 2017a,b; Chen et al., 2017). As a consequence of rate-dependency, delayed fracture might result when soft materials are subjected to a constant load, differently from crystalline solids where fracture usually occurs instantaneously at a well-defined critical strength (Bonn, 1998). Adding complexity to the analysis, we should also consider that when cutting or pearcing is studied in relation to real biological tissues, such as the human skin, an anisotropic and heterogeneous nature is often displayed.

Most studies concerning cutting and puncturing of soft materials deal with the penetration of biological tissues by means of needles, combining experimental measurements of the mechanical properties with numerical analyses. Studying the deep penetration of a needle into the skin, Shergold and Fleck (Shergold and Fleck, 2004, 2005) recorded the load-displacement curves for different indenters, and observed that the crack geometry is sensitive to the indenter tip geometry and to the material properties of the soft solid. Detailed numerical modelling by means of the finite element (FE) method are often employed as a complement to experimental measurements, enabling a better understanding of the complex interaction between the tool and the soft matter (DiMaio and Salcudean, 2003; Oldfield et al., 2013).

In the present paper, a two-dimensional analytical LEFM model, proposed by the authors (Ståhle et al., 2017; Terzano et al., 2018; Spagnoli et al., 2018), is exploited to describe the mechanism of Mode I fracture occurring in a plane orthogonal to the axis of a sharp tipped circular rigid needle while its penetration occurs. Finite element analyses are carried out to assess the model proposed. Closed form solutions for calculating the dimensionless penetration force as a function of the relative fracture toughness of the material are obtained. Although the study is conditioned by the strong assumption of a linear elastic material behaviour, it might represent a reference for further investigations where the non-linear elastic behaviour of soft materials is fully taken into account.

Some experimental tests are carried out by using additively manufactured penetrating tools and target materials.

2. Mechanics of puncturing

The mechanics of a foreign object piercing a target solid is characterised by two stages: an initial stage of *indentation* and a subsequent stage of *deep penetration*. In the former, the tip of the foreign object is in contact with the target solid, which accumulates strain energy while the penetration progresses; indentation stage terminates when an energetically favorable mechanism of laceration takes place in the target solid (Fregonese and Bacca, 2021). This mechanism features the development of a crack linearly increasing its length with the penetration depth of the foreign object. According to Shergold and Fleck (2004), for soft materials either mode-II crack rings or mode-I planar cracks develop for flat-bottomed punch and sharp-tipped punch, respectively.

In the present paper, a rigid sharp-tipped punch (needle) is assumed to penetrate a large soft solid along the *z* direction (Figure 1). Let us introduce the energy-based formulation of the puncturing process; the increment of external work generated by the puncturing force is consumed by different contributions: the strain energy, the work of fracture, and the frictional dissipation. The general incremental form of the energy balance is

$$\mathrm{d}U_{ext} = \mathrm{d}U_s + \mathrm{d}U_G + \mathrm{d}U_f \tag{1}$$

where $\mathrm{d}U_{ext}$ is the external work input, $\mathrm{d}U_s$ is the strain energy variation in the solid, $\mathrm{d}U_G$ is the energy spent to advance the crack, and $\mathrm{d}U_f$ is the energy dissipated due to friction at the needle-material interface. The force F is exerted on the needle to penetrate a small amount dD, so that $\mathrm{d}U_{ext} = F\mathrm{d}D$.
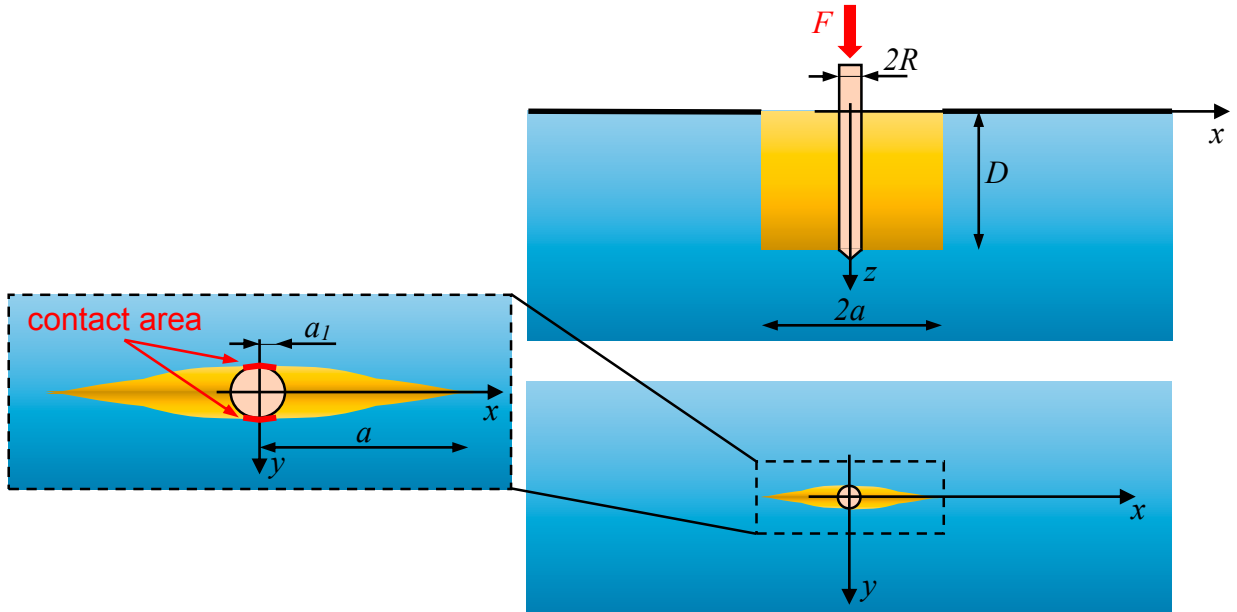
Fig. 1. Sketch of the Mode I crack mechanism of puncturing in the deep penetration of a rigid circular sharp-tipped punch.

Following the initial stage of indentation, deep penetration is characterised by a steady-state condition, where a Mode I planar crack of size $2a \times D$ propagates (the crack area is defined by the region $-a \leq x \leq a$ and $0 \leq z \leq D$). The energy G available per unit increase in area of one fracture surface (referred to the undeformed configuration), $dA = 2a da$, is given by

$$G = \frac{F}{2a} - \frac{dU_s}{2a dD} - \frac{dU_f}{2a dD} \tag{2}$$

Within the framework of LEFM, the crack driving energy of Eq. (2) can be expressed as $G = K_I^2/E^*$ by means of Irwin's relation, where K is the stress intensity factor (SIF) and $E^* = E/(1 - v^2)$ is the Young's modulus of the material under plane strain condition (v = Poisson's ratio). In the case of incompressibile material ($v = 0.5$) we have $E = 3\mu$ and $E^* = 4\mu$, being μ the shear modulus. Crack propagation occurs when either the fracture energy or the stress intensity factor reaches the critical values $G = G_c$ or $K = K_c$, which commonly define the fracture toughness of the material.

3. Mode I penetration mechanism

3.1. LEFM analytical model

In this section, a theoretical model of cutting based on LEFM is briefly reviewed. Small-scale yielding is assumed at the crack tip, along with frictionless contact at needle-material interface and small strain conditions. Details of the complete formulation can be found elsewhere (Ståhle et al., 2017; Terzano et al., 2018; Spagnoli et al., 2018), where the cutting tool geometry is described by a rigid elliptical wedge.

A rigid needle of circular cross-section is inserted into the target material, exemplified by a semi-infinite linearly elastic solid. Consider a section of the solid normal to the needle axis, corresponding to any plane of equation $z = \bar{z}$ with $\bar{z} \leq D$, Figure 1. The resulting two-dimensional problem is characterised by plane strain condition. The cross-section profile of the needle is expressed by $h(x) = \sqrt{R^2 - x^2}$, where R is the radius of its cross section.
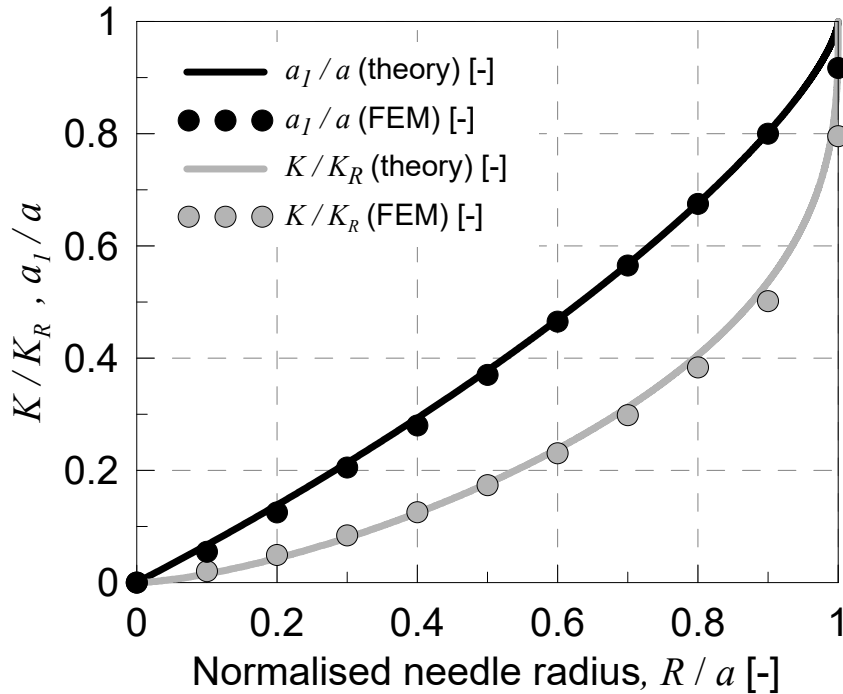
Fig. 2. Theoretical and FE distribution of relative SIF and contact length versus relative radius of the needle.

It has been shown in (Ståhle et al., 2017) that the crack surfaces detach from the needle profile at a coordinate $x = a_1$, so that the cut is traction free for $a_1 \leq x < a$ (see Fig. 1). From the solution of a boundary value problem (Terzano et al., 2018), the position of the point of separation a_1 and the stress intensity factor at the crack tip K, are obtained. The results are plotted in Figure 2, against the normalised needle radius R/a. The SIF K is normalised with respect to K_R, namely the stress intensity factor related to the needle filling the entire crack ($R/a = 1$). This is defined as

$$K_R = \frac{E^*}{2} \sqrt{\pi R} \tag{3}$$

The SIF K_R turns out to be proportional to the square root of the radius of curvature at the crack tip (when $R/a = 1$, no detachment length $a - a_1$ develops).

For a given radius of the needle, depending on the toughness of the material, a planar crack of semi-length a forms so that $K = K_c$ at the crack tips. In other words, the critical value of the relative radius, corresponding to the ratio between the radius and the critical crack semi-length, R/a_c, is determined (along with the critical value of the contact relative semi-length a_1/a_c) from the curve of $R/a - K/K_R$ in Figure 2 by posing $K = K_c$. Note that, according to the present model, the needle penetration produces the crack development provided that $R \geq R_c$, where R_c is a material-based length parameter, defined as

$$R_c = \frac{4}{\pi} \left(\frac{K_c}{E^*} \right)^2 \tag{4}$$

When the needle penetrates for a depth D, strain energy accumulates in the target material due to its deformation induced by the contact pressure at the needle-solid interface. As a first rough estimation, the contact pressure might be described by the Hertzian theory of non-conforming contacts. Accordingly, the contact pressure tends to be null at the boundaries of the contact region ($|x| = a_1$) and maximum in the centre ($x = 0$), with the resultant P dependent on the contact length $2a_1$. Specifically, the resultant of the contact pressure acting over the area $2a_1 \times D$ is (Johnson, 1987)

$$P = \frac{\pi E^* a_1{}^2}{4R} D \tag{5}$$

where R is the radius of the needle.

Making use of Eq. (3) to express K_R, it turns out that

$$P = \frac{1}{2} \sqrt{\frac{\pi}{R}} \frac{a_1^2}{R} K_R D \tag{6}$$

On the other hand, by assuming a uniform contact pressure equal to $E^*/2$ (a remote tensile stress $\sigma_0 = E^*/2$ acting on large plate with a central crack $2a$ produces a maximum crack flank displacement equal to R) we get (Terzano et al., 2018)

$$P = 2a_1 \frac{E^*}{2} D = \frac{2}{\sqrt{\pi R}} a_1 K_R D \tag{7}$$

Finally, according to Clapeyron's theorem, the following relation holds

$$\frac{dU_s}{dD} = \frac{P}{D} R \tag{8}$$

Results of the normalised strain energy per unit thickness considering the two distributions above of contact pressure are illustrated in Figure 3 as a function of the relative needle radius R/a.

3.2. Comparison with FE

A section of the target solid at $z = \bar{z} \leq D$ is considered. Due to symmetry conditions, only a quarter of this section is described by finite element (FE) models. A large solid is considered, so that the quarter plate has dimensions $20a \times 20a$ being a the crack semi-length. Plane strain 8-node isoparametric elements are used. A suitable mesh is adopted with minimum size of the eleements near the crack equal to $a/100$. Non-linear springs (with a penalty compressive stiffness and nearly zero stiffness in tension) are used to simulate the unilateral contact between needle and target material. Incremental static non-linear analyses are carried out by keeping a constant and varying R ($R/a = 0.1, 0.2, ..., 1$). The needle is pushed against the target material by an incremental displacement from 0 to R.

Comparisons between FE results and theory in terms of contact length a_1/a, SIF K/K_R and strain energy U_s are presented in Figures 2 and 3. A perfect agreement between theoretical and numerical results is observed for a_1/a and K/K_R, while the best approximation of the strain energy distribution is obtained by considering the Hertzian contact pressure.
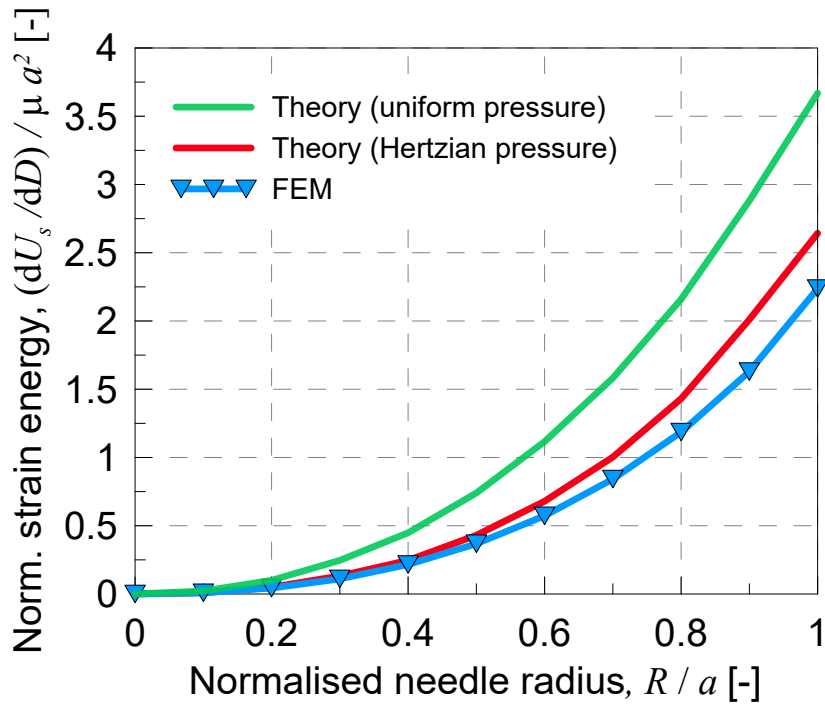
Fig. 3. Theoretical and FE distribution of normalised strain energy versus relative radius of the needle.

4. Results in terms of penetration force

As it is shown in Figure 3, the contact pressure is well described by the Hertzian distribution. Hence, by inserting Eq. 5 in Eq. 8, we get (the shear modulus μ is equal to $E/3$ and to $E^*/4$ for a linear elastic incompressible material)

$$\frac{dU_s}{dD} = \pi\mu a_1^2 \tag{9}$$

Considering that $dU_G/dD = 2aG_c$, at the onset of deep penetration (the frictional contribution is not considered), the penetration force F_p is equal to

$$F_p = \pi\mu a_1^2 + 2aG_c \tag{10}$$

This expression can be conveniently written in a dimensionless form as (Figure 4)

$$\frac{F_p}{\mu R^2} = \pi\left(\frac{a_1}{a_c}\right)^2\left(\frac{a_c}{R}\right)^2 + 2\frac{G_c}{\mu R}\left(\frac{a_c}{R}\right) \tag{11}$$
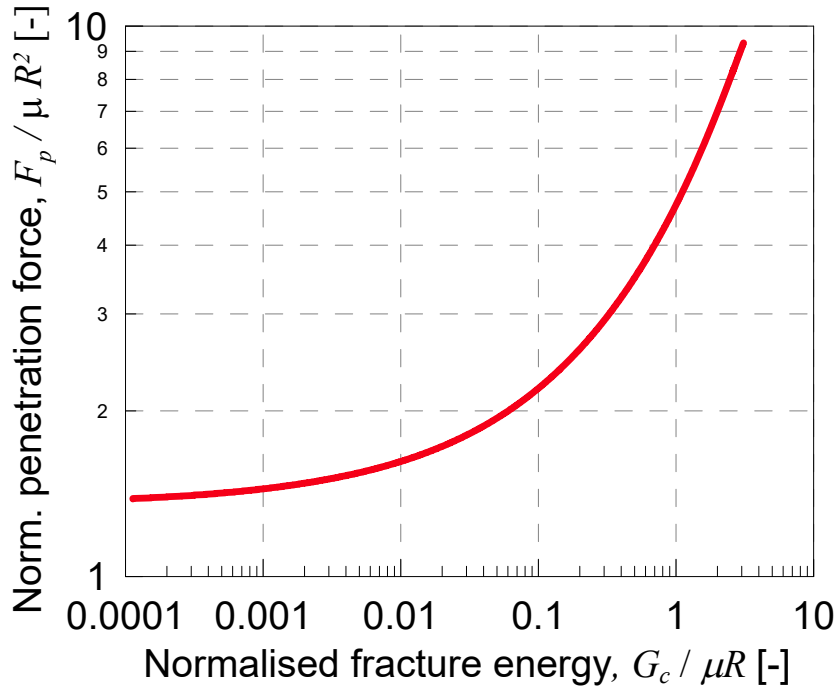
Fig. 4. Theoretical value of dimensionless penetration force as a function of the relative fracture energy of the target material.

The values of a_1/a_c and R/a_c can be obtained from the theoretical results illustrated in Figure 2, for a given value of fracture toughness $K_c = 2\sqrt{G_c\mu} = K_R\sqrt{G_c}/\sqrt{\mu\pi R}$. Note that, according to the present model, the Mode I penetration mechanism can occur only if $G_c/(\mu R) \le \pi$, but if a crack failure criterion different from that of LEFM is used, higher values of the normalised fracture energy might be allowed.

For a given material and needle geometry, one calculates $G_c/\mu R$ and hence K_c/K_R ($K_c/K_R = \sqrt{G_c/\mu R}\sqrt{1/\pi}$). Then, from the curves of Figure 2 the critical ratios R/a_a and a_1/a_c can be determined. Finally, the dimensionless penetration force $F_p/\mu R^2$ is given by Eq. 11.

5. Conclusion and future work

This paper shows the validity of a recently proposed model, based on LEFM concepts, to describe the penetration mechanism of a rigid circular needle into a soft target material. The needle is assumed to have a sharp tip so that penetration is governed by the development of a planar Mode I crack exposed to the contact pressure at the needle-material interface. The theoretical model is verified by running non-linear FE models where the unilateral contact between the needle and the target material is described. A simple closed-form expression is then obtained for the dimensionless penetration force as a function of the relative fracture toughness of the material.

The present work might offer a first insight on the mechanics of puncturing in soft materials, thanks to its simplified assumptions. However, further work is needed to address relevant aspects, such as: (i) hyperelastic models to describe the finite strain deformation of soft materials; (ii) failure and fracture conditions in soft materials; (iii) development of different mechanisms (e.g. hole expansion) during penetration of sharp tipped needles in soft materials.

6. Acknowledgments

References

Anderson, P.S., 2018. Making a point: shared mechanics underlying the diversity of biological puncture. Journal of Experimental Biology 221, jeb187294.

Bezek, L.B., Chatham, C.A., Dillard, D.A., Williams, C.B., 2022. Mechanical properties of tissue-mimicking composites formed by material jetting additive manufacturing. Journal of the Mechanical Behavior of Biomedical Materials 125, 104938.

Bonn, D., 1998. Delayed Fracture of an Inhomogeneous Soft Solid. Science 280, 265–7. doi:10.1126/science.280.5361.265.

Brighenti, R., Spagnoli, A., Carpinteri, A., Artoni, F., 2017a. Defect tolerance at various strain rates in elastomeric materials: An experimental investigation. Engineering Fracture Mechanics 183, 79–93. doi:10.1016/j.engfracmech.2017.05.001.

Brighenti, R., Vernerey, F.J., Artoni, F., 2017b. Rate-dependent failure mechanism of elastomers. International Journal of Mechanical Sciences 130, 448–57. doi:10.1016/j.ijmecsci.2017.05.033.

Chen, C., Wang, Z., Suo, Z., 2017. Flaw sensitivity of highly stretchable materials. Extreme Mechanics Letters 10, 50–7. doi:10.1016/j.eml.2016.10.002.

DiMaio, S., Salcudean, S., 2003. Needle insertion modeling and simulation. IEEE Transactions on Robotics and Automation 19, 864–75. doi:10.1109/TRA.2003.817044.

Fregonese, S., Bacca, M., 2021. Piercing soft solids: A mechanical theory for needle insertion. Journal of the Mechanics and Physics of Solids 154, 104497.

Frick, T.B., Marucci, D.D., Cartmill, J.A., Martin, C.J., Walsh, W.R., 2001. Resistance forces acting on suture needles. Journal of Biomechanics 34, 1335–40. doi:10.1016/S0021-9290(01)00099-9.

Goh, S.M., Charalambides, M.N., Williams, J.G., 2005. On the mechanics of wire cutting of cheese. Engineering Fracture Mechanics 72, 931–46. doi:10.1016/J.ENGFRACMECH.2004.07.015.

Johnson, K.L., 1987. Contact Mechanics. Cambridge University Press.

Kundanati, L., Guarino, R., Menegon, M., Pugno, N.M., 2020. Mechanics of snake biting: Experiments and modelling. Journal of the mechanical behavior of biomedical materials 112, 104020.

McGorry, R.W., Dowd, P.C., Dempsey, P.G., 2003. Cutting moments and grip forces in meat cutting operations and the effect of knife sharpness. Applied Ergonomics 34, 375–82. doi:10.1016/S0003-6870(03)00041-3.

Oldfield, M., Dini, D., Giordano, G., Rodriguez y Baena, F., 2013. Detailed finite element modelling of deep needle insertions into a soft tissue phantom using a cohesive approach. Computer Methods in Biomechanics and Biomedical Engineering 16, 530–43. doi:10.1080/10255842.2011.628448.

Shergold, O.A., Fleck, N.A., 2004. Mechanisms of deep penetration of soft solids, with application to the injection and wounding of skin. Proceedings of the Royal Society A: Mathematical, Physical and Engineering Sciences 460, 3037–58. doi:10.1098/rspa.2004.1315.

Shergold, O.A., Fleck, N.A., 2005. Experimental Investigation Into the Deep Penetration of Soft Solids by Sharp and Blunt Punches, With Application to the Piercing of Skin. Journal of Biomechanical Engineering 127, 838–48. doi:10.1115/1.1992528.

Spagnoli, A., Terzano, M., Brighenti, R., Artoni, F., Ståhle, P., 2018. The fracture mechanics in cutting: a comparative study on hard and soft polymeric materials. International Journal of Mechanical Sciences 148, 554–564.

Ståhle, P., Spagnoli, A., Terzano, M., 2017. On the fracture processes of cutting. Procedia Structural Integrity 3, 468–476.

Takabi, B., Tai, B.L., 2017. A review of cutting mechanics and modeling techniques for biological materials. Medical Engineering & Physics 45, 1–14. doi:10.1016/J.MEDENGPHY.2017.04.004.

Terzano, M., Dini, D., Rodriguez y Baena, F., Spagnoli, A., Oldfield, M., 2020. An adaptive finite element model for steerable needles. Biomechanics and Modeling in Mechanobiology 19, 1809–1825.

Terzano, M., Spagnoli, A., Dini, D., Forte, A.E., 2021. Fluid–solid interaction in the rate-dependent failure of brain tissue and biomimicking gels. Journal of the Mechanical Behavior of Biomedical Materials 119, 104530.

Terzano, M., Spagnoli, A., Ståhle, P., 2018. A fracture mechanics model to study indentation cutting. Fatigue & Fracture of Engineering Materials & Structures 41, 821–30. doi:10.1111/ffe.12750.

Williams, J.G., 2015. Stress at a distance fracture criteria and crack self-blunting in rubber. International Journal of Non-Linear Mechanics 68, 33–6. doi:10.1016/j.ijnonlinmec.2014.06.008.